Tracking of Signal Subspace Projectors

Wolfgang Utschick

***Abstract*—A new subspace tracking approach that directly operates on the projection matrix onto the signal subspace instead of tracking its unitary eigenbasis is proposed. Therefore, the difficulties arising from introducing a calculus on the manifold of projection matrices are overcome by a proper parameterization of the projectors. Simulation results are presented from the field of angular frequency retrieval in array signal processing.**

***Index Terms*—DSP implementation, parameterization, projection matrices, steepest descent optimization, subspace tracking, unitary rotations.**

I. Introduction

THE eigendecomposition of the data space into a signal subspace and a noise subspace plays an important role in subspace based methods in signal processing, e.g., high-resolution methods for direction-of-arrival (DOA) finding and parameter estimation like MUSIC [1], the minimum-norm method [2], ESPRIT [3], and weighted subspace fitting [4]. Subspace estimation is a very costly numerical task, especially in a time-variant scenario, where the subspace changes with time and, therefore, has to be computed over and over again. However, tracking the subspace may be a solution.

In [5], the authors presented a thorough overview of most of the adaptive algorithms for subspace tracking. Thus, the subspace tracking techniques can be categorized into three families (cf. [6]):

i) classical eigenvalue decomposition and singular value decomposition methods modified for use in adaptive processing (e.g., [7]);
ii) variations of rank-one updating algorithms (e.g., [8], [9]);
iii) algorithms that consider the eigenvalue/singular value decomposition as a constrained or unconstrained optimization problem which can be adaptively processed by means of gradient based methods (e.g., [6], [10], and [11]).

A further feature of the algorithms concerns whether the methods are discussed in a block processing context or in a sequential data processing mode. The latter performs an updating of the eigenbasis recursively on the arrival of a new data snapshot.

From the numerical complexity point of view, the different algorithms are distinguished between methods requiring $\mathcal{O}(M^2d), \mathcal{O}(M^2), \mathcal{O}(Md^2)$, or $\mathcal{O}(Md)$ operations every update (sequential mode), where M is the input vector dimension, and d is the number of desired eigencomponents.

In this work, the variety of type-iii approaches is extended by a tracking method that directly operates on the unique projection matrix onto the signal subspace instead of tracking its unitary eigenbasis.

A common feature of subspace estimation is that the computed basis of the signal subspace is not essentially unique. Otherwise, the notation of subspaces by means of a projector is well defined. The development of the algorithm will be demonstrated in a block processing context.

Manuscript received May 15, 2000; revised January 2, 2002. The associate editor coordinating the review of this paper and approving it for publication was Dr. Brian Sadler.

The author is with the Institute for Circuit Theory and Signal Processing, Munich University of Technology, Munich, Germany (e-mail: utschick@nws.ei.tum.de).

Publisher Item Identifier S 1053-587X(02)02397-8.

II. Data Model

Assume that there are d narrowband signals having the same center frequency f_0 and being characterized by their complex envelopes $s_i(t) \in \mathbb{C}, 1 \leq i \leq d$, simultaneously sampled according to M different linear combinations $x_j(t) \in \mathbb{C}, 1 \leq j \leq M$ of the $s_i(t)$. In the following, we always consider a blockwise processing of the sampled data $\boldsymbol{x}$. To this end, let the noisy measurement matrix $\boldsymbol{X}$ be constituted by $\boldsymbol{X} \triangleq [\boldsymbol{x}_1 \ldots \boldsymbol{x}_N] \in \mathbb{C}^{M\times N}$, where $\hat{\boldsymbol{R}}_x \triangleq \boldsymbol{X}\boldsymbol{X}^H$ denotes the sample estimate[1] of $\boldsymbol{R}_x \triangleq E[\boldsymbol{x}\boldsymbol{x}^H] \in \mathbb{C}^{M\times M}$. Let the eigendecomposition (ED) of $\hat{\boldsymbol{R}}_x$ be equal to $\hat{\boldsymbol{R}}_x = \hat{\boldsymbol{U}}\hat{\boldsymbol{\Lambda}}\hat{\boldsymbol{U}}^H$, where $\hat{\boldsymbol{\Lambda}} \triangleq \operatorname{diag}[\hat{\lambda}_1, \ldots, \hat{\lambda}_M]$ contains the real-valued eigenvalues of $\hat{\boldsymbol{R}}_x$, and the unitary matrix $\hat{\boldsymbol{U}}$ contains the corresponding eigenvectors. For convenience, the eigenvalues of $\boldsymbol{R}_x$ are arranged in a descending order: $\lambda_1 \geq \lambda_2 \geq \cdots \geq \lambda_d > \lambda_{d+1} = \cdots = \lambda_M = \sigma^2$, and we define $\boldsymbol{\Lambda}_s \triangleq \operatorname{diag}[\lambda_1, \ldots, \lambda_d], \boldsymbol{\Lambda}_n \triangleq \operatorname{diag}[\lambda_{d+1}, \ldots, \lambda_M]$. Accordingly, the eigenvector matrix $\boldsymbol{U}$ is decomposed as $\boldsymbol{U} \triangleq [\boldsymbol{U}_s\boldsymbol{U}_n]$, where $\boldsymbol{U}_s \triangleq [\boldsymbol{u}_1 \ldots \boldsymbol{u}_d]$ contains the first d columns of $\boldsymbol{U}$, and $\boldsymbol{U}_n \triangleq [\boldsymbol{u}_{d+1} \ldots \boldsymbol{u}_M]$ is equal to the further columns, respectively. Thus, we express $\boldsymbol{R}_x$ as

$$\boldsymbol{R}_x = \boldsymbol{U}_s\boldsymbol{\Lambda}_s\boldsymbol{U}_s^H + \boldsymbol{U}_n\boldsymbol{\Lambda}_n\boldsymbol{U}_n^H. \tag{1}$$

III. Tracking Using Projection Approximation

Projection approximation subspace tracking (PAST) [6] is one successful subspace tracking algorithm due to its simplicity and efficiency. Consider the following optimization criterion:

$$J(\boldsymbol{W}) \triangleq E[\|\boldsymbol{x} - \boldsymbol{W}\boldsymbol{W}^H\boldsymbol{x}\|^2] \tag{2}$$

where $\boldsymbol{W} \in \mathbb{C}^{M\times d}$ is a full-rank matrix to be found. The following theorem states the very desirable properties of the criterion $J(\boldsymbol{W}) \in \mathbb{R}$.

[1] $\boldsymbol{x}^H \equiv (\boldsymbol{x}^*)^T \equiv \boldsymbol{x}^{T,*}$ denotes the conjugate transpose of $\boldsymbol{x}$.

Theorem 1: The matrix $\boldsymbol{W}$ is a stationary point of $J(\boldsymbol{W})$ if and only if $\boldsymbol{W} = \boldsymbol{U}_d\boldsymbol{Q}$, where $\boldsymbol{U}_d \in \mathbb{C}^{M\times d}$ contains any d distinct eigenvectors of $\boldsymbol{R}_x$, and $\boldsymbol{Q} \in \mathbb{C}^{d\times d}$ is an arbitrary unitary matrix. At each stationary point, $J(\boldsymbol{W})$ is equal to the sum of eigenvalues whose eigenvectors are not involved in $\boldsymbol{U}_d$.

Moreover, all stationary points of $J(\boldsymbol{W})$ are saddle points, except when $\boldsymbol{U}_d = \boldsymbol{U}_s$. In this case, $J(\boldsymbol{W})$ attains the global minimum. That is

$$\boldsymbol{W}_{\text{opt}} = \boldsymbol{U}_s\boldsymbol{Q} = \arg\min J(\boldsymbol{W}) \tag{3}$$

$$J(\boldsymbol{W}_{\text{opt}}) = \lambda_{d+1} + \cdots + \lambda_M = (M-d)\sigma^2. \tag{4}$$

Proof: See [6]. ∎

Note that the minimization of $J(\boldsymbol{W})$ with respect to $\boldsymbol{W}$ represents an unconstrained optimization problem that may be solved in a straightforward manner. On the basis of Theorem 1, a few efficient algorithms can be developed for subspace tracking [6]. A computationally efficient algorithm for blockwise available data $\boldsymbol{X} \in \mathbb{C}^{M\times N}$ is the following stochastic gradient algorithm (cf. [12], [13]):

$$\begin{aligned}\boldsymbol{Y}[t] &\leftarrow \boldsymbol{W}^H[t-1]\boldsymbol{X}[t]\\ \boldsymbol{W}[t] &\leftarrow \boldsymbol{W}[t-1] + \mu[\boldsymbol{X}[t] - \boldsymbol{W}[t-1]\boldsymbol{Y}[t]]\boldsymbol{Y}^H[t]\end{aligned} \tag{5}$$

where $\mu > 0$ and t are the step-size to be properly selected and the iteration number, respectively.

IV. Projection Matrices

It is interesting to note that by virtue of the global minimizer $\boldsymbol{W}_{\text{opt}} \in \mathbb{C}^{M\times d}$ of the criterion $J(\boldsymbol{W}) \in \mathbb{R}$, the matrix that defines the projection onto the signal subspace $\mathcal{S}$ can be constructed as

$$\boldsymbol{P}_{\text{opt}} \triangleq \boldsymbol{W}_{\text{opt}}\boldsymbol{W}_{\text{opt}}^H = \boldsymbol{U}_s\boldsymbol{Q}(\boldsymbol{U}_s\boldsymbol{Q})^H = \boldsymbol{U}_s\boldsymbol{U}_s^H \tag{6}$$

since $\boldsymbol{Q}\boldsymbol{Q}^H = \boldsymbol{I}_d$. This motivates us to consider replacing $\boldsymbol{W}\boldsymbol{W}^H$ in $J(\boldsymbol{W})$ by the matrix argument $\boldsymbol{P} \in \mathbb{C}^{M\times M}$, which gives the following criterion expressed[2] in terms of $\boldsymbol{P} \in \mathbb{C}^{M\times M}$:

$$\begin{aligned}\tilde{J}(\boldsymbol{P}) &\triangleq E[\|\boldsymbol{x} - \boldsymbol{P}\boldsymbol{x}\|^2]\\ &= \text{tr}(\boldsymbol{R}_x - \boldsymbol{R}_x\boldsymbol{P} - \boldsymbol{R}_x\boldsymbol{P}^H + \boldsymbol{R}_x\boldsymbol{P}^H\boldsymbol{P}).\end{aligned} \tag{7}$$

Note that in (7), we do not exploit any properties of the projector matrix $\boldsymbol{P}$. However, using the properties $\boldsymbol{U}_s^H\boldsymbol{U}_s = \boldsymbol{I}_d, \boldsymbol{U}_s^H\boldsymbol{U}_n = \boldsymbol{0}$ and, thus, $\boldsymbol{R}_x\boldsymbol{P} = \boldsymbol{R}_x\boldsymbol{U}_s\boldsymbol{U}_s^H = \boldsymbol{U}_s\boldsymbol{\Lambda}_s\boldsymbol{U}_s^H$, the criterion $\tilde{J}(\boldsymbol{P})$ will take on the value $(M-d)\sigma^2$ from (4) in Theorem 1. Nevertheless, $\boldsymbol{P} = \boldsymbol{U}_s\boldsymbol{U}_s^H$ is neither a stationary point nor a global minimizer of $\tilde{J}(\boldsymbol{P})$. This is due to the fact that $\tilde{J}(\boldsymbol{P})$ may be considered to be an unstructured version of $J(\boldsymbol{W})$. Obviously, unlike the criterion $J(\boldsymbol{W})$ in (2), working with the unconstrained $\tilde{J}(\boldsymbol{P})$ does not automatically give rise to a solution for the subspace projection matrix. Due to the above reasons, to update the projection matrix, additional constraints must be imposed on $\boldsymbol{P}$ to form the constrained minimization problem:

$$\begin{aligned}&\min \tilde{J}(\boldsymbol{P})\\ &\text{subject to}\\ &\quad \text{i)}\quad \text{rank}(\boldsymbol{P}) = d \quad \text{(low-rank)}\\ &\quad \text{ii)}\quad \boldsymbol{P}^2 = \boldsymbol{P} \quad \text{(idempotent)}\\ &\quad \text{iii)}\quad \boldsymbol{P}^H = \boldsymbol{P}\end{aligned} \tag{8}$$

and accordingly

$$\tilde{J}(\boldsymbol{P}) \triangleq E[\|\boldsymbol{x} - \boldsymbol{P}\boldsymbol{x}\|^2] = \text{tr}(\boldsymbol{R}_x) - \text{tr}(\boldsymbol{R}_x\boldsymbol{P}). \tag{9}$$

The main problem of tracking the matrix $\boldsymbol{P}$ is given by the constraints in (8). A gradient descent algorithm to minimize the criterion seems to be inadequate for minimization of $\tilde{J}(\boldsymbol{P})$ because any increment $\Delta\boldsymbol{P}$ to $\boldsymbol{P}$ destroys the properties of being an projection matrix. This is solely due to an inadequate parameterization of the manifold of projection matrices. To this end, we introduce the following lemma and a theorem, which will help us to find a proper parameterization of projectors.[3]

Lemma 1: Given the M-dimensional plane unitary rotation matrices $\boldsymbol{G}^{k,\ell}(\phi_{k,\ell}, \sigma_{k,\ell}) \in \mathbb{C}^{M\times M}$, i.e., the *Givens rotors* [7], [15], [16] with the characteristic 2×2 submatrix

$$\boldsymbol{G}^{k,\ell}_{\left[\begin{smallmatrix}k,k & k,\ell\\ \ell,k & \ell,\ell\end{smallmatrix}\right]} \triangleq \begin{bmatrix}\cos(\phi_{k,\ell}) & -e^{-j\sigma_{k,\ell}}\cdot\sin(\phi_{k,\ell})\\ e^{j\sigma_{k,\ell}}\cdot\sin(\phi_{k,\ell}) & \cos(\phi_{k,\ell})\end{bmatrix} \tag{10}$$

and the diagonal matrix

$$\boldsymbol{\Gamma}(\boldsymbol{\xi}) = \begin{bmatrix}e^{j\xi_1} & & & \\ & e^{j\xi_2} & & \\ & & \ddots & \\ & & & e^{j\xi_M}\end{bmatrix} \tag{11}$$

any M-dimensional unitary matrix $\boldsymbol{Q} \in \mathbb{C}^{M\times M}$ can be expressed as[4]

$$\boldsymbol{Q} = \boldsymbol{\Gamma}(\boldsymbol{\xi})\cdot\boldsymbol{G}(\boldsymbol{\phi},\boldsymbol{\sigma}) \tag{12}$$

where the unitary matrix

$$\boldsymbol{G}(\boldsymbol{\phi},\boldsymbol{\sigma}) \triangleq \prod_{k=M-1}^{1}\prod_{\ell=k+1}^{M}\boldsymbol{G}^{k,\ell}(\phi_{k,\ell},\sigma_{k,\ell}). \tag{13}$$

The vectors $\boldsymbol{\phi},\boldsymbol{\sigma}$, and $\boldsymbol{\xi}$ compose the parameters $\boldsymbol{\phi} \triangleq [\ldots,\phi_{k,\ell},\ldots]^T, \boldsymbol{\sigma} \triangleq [\ldots,\sigma_{k,\ell},\ldots]^T$, and $\boldsymbol{\xi} \triangleq [\ldots,\xi_m,\ldots]^T$, where the indices count from $k = M-1, M-2, \ldots, 1, \ell =$

[2]Note that $E[\boldsymbol{x}^H\boldsymbol{P}\boldsymbol{x}] \equiv \text{tr}(\boldsymbol{P}E[\boldsymbol{x}\boldsymbol{x}^H]) \equiv \text{tr}(E[\boldsymbol{x}\boldsymbol{x}^H]\boldsymbol{P})$, where tr(•) denotes the trace of the matrix argument.

[3]The use of a different parameterization of matrices for the sake of numerical optimization of matrix functions has been found in [14].

[4]Example of a three-dimensional (3-D) unitary matrix

$$\boldsymbol{Q} = \text{diag}[e_1,e_2,e_3]\times\begin{bmatrix}1 & 0 & 0\\ 0 & c_{2,3} & -s_{2,3}\\ 0 & s_{2,3} & c_{2,3}\end{bmatrix}\times\begin{bmatrix}c_{1,2} & -s_{1,2} & 0\\ s_{1,2} & c_{1,2} & 0\\ 0 & 0 & 1\end{bmatrix}\begin{bmatrix}c_{1,3} & 0 & -s_{1,3}\\ 0 & 1 & 0\\ s_{1,3} & 0 & c_{1,3}\end{bmatrix}$$

where $c_{k,\ell} = \cos(\phi_{k,\ell}), \pm s_{k,\ell} = \pm e^{\pm i\sigma_{k,\ell}}\cdot\sin(\phi_{k,\ell})$, and $e_m = e^{j\xi_m}$.

$k+1, k+2, \ldots, M$, and $m = 1, \ldots, M$, respectively. Therefore, the bounded and closed space of M-dimensional unitary matrices $\boldsymbol{Q}$ can be parameterized by means of overall M^2 parameters $\phi_{k,\ell} \in [-\pi, +\pi), \sigma_{k,\ell} \in [-(\pi/2), +(\pi/2)]$, and $\xi_m \in [-(\pi/2), +(\pi/2)]$.

Proof: The decomposition of a complex matrix by elementary plane unitary rotations was already given in [15]; see also [17]. For the special form of the parameterization in Lemma 1, see also [14] and [18], where another [19] has been cited. ■

Theorem 2: Given $\mathcal{P}$, the space of M-dimensional projection matrices $\boldsymbol{P} \in \mathbb{C}^{M \times M}$ of rank$(\boldsymbol{P}) = d$, then, for all $\delta > 0$ and all $\boldsymbol{P}_u \in \mathcal{P}$, there exists $\epsilon > 0$ such that for all $\boldsymbol{P}_v \in \mathcal{U}_\epsilon(\boldsymbol{P}_u) \subset \mathcal{P}$, there exist parameters $\boldsymbol{\phi}$ and $\boldsymbol{\xi}$ of $\boldsymbol{Q}$ such that [5]

$$||\boldsymbol{P}_v - \boldsymbol{Q}\boldsymbol{P}_u\boldsymbol{Q}^H||_2 < \delta \tag{14}$$

holds, where

$$\boldsymbol{Q} \triangleq \boldsymbol{\Gamma}(\boldsymbol{\xi}) \cdot \boldsymbol{G}(\boldsymbol{\phi}) \tag{15}$$

and the matrices $\boldsymbol{\Gamma}(\boldsymbol{\xi}) \in \mathbb{C}^{M \times M}$ and $\boldsymbol{G}(\boldsymbol{\phi}) \triangleq \boldsymbol{G}_r(\boldsymbol{\phi}) \triangleq \prod_{k=M-1}^{1} \prod_{\ell=k+1}^{M} \boldsymbol{G}_r^{k,\ell}(\phi_{k,\ell}, 0) \in \mathbb{R}^{M \times M}$ are diagonal and orthonormal, respectively. Therefore, $\boldsymbol{G}_r(\phi_{k,\ell}, 0)$ denotes the *Givens rotor* from Lemma 1, where $\sigma_{k,\ell} = 0$. The $\mathcal{U}_\epsilon(\boldsymbol{P}_u)$ denotes the open set of projection matrices given by the ϵ ball

$$\mathcal{U}_\epsilon(\boldsymbol{P}_u) \triangleq \{\tilde{\boldsymbol{P}} \in \mathcal{P} \quad : \quad ||\tilde{\boldsymbol{P}} - \boldsymbol{P}_u||_2 < \epsilon\}. \tag{16}$$

Proof: See Appendix B. ■

Corollary 1: Given $\mathcal{P}$, the space of M-dimensional projection matrices $\boldsymbol{P} \in \mathbb{R}^{M \times M}$ of rank$(\boldsymbol{P}) = d$, then, for all $\delta > 0$ and all $\boldsymbol{P}_u \in \mathcal{P}$, there exists $\epsilon > 0$ such that for all $\boldsymbol{P}_v \in \mathcal{U}_\epsilon(\boldsymbol{P}_u) \subset \mathcal{P}$, there exist parameters $\boldsymbol{\phi}$ of $\boldsymbol{G}$, such that

$$||\boldsymbol{P}_v - \boldsymbol{G}\boldsymbol{P}_u\boldsymbol{G}^T||_2 < \delta \tag{17}$$

holds, with the orthonormal matrix $\boldsymbol{G} \triangleq \boldsymbol{G}_r(\boldsymbol{\phi}) \in \mathbb{R}^{M \times M}$.

Proof: If $\boldsymbol{P}_v$ and $\boldsymbol{P}_u$ are elements of $\mathbb{R}^{M \times M}$, the transformation matrix $\boldsymbol{Q}$ in Theorem 2 is an element of $\mathbb{R}^{M \times M}$ as well. Hence, according to Lemma 1, the parameters ξ_m and $\sigma_{k,\ell}$ of $\boldsymbol{Q}$ must be equal to zero for all $k, \ell, m = 1, \ldots, M$, and thus, $\boldsymbol{\Gamma} = \boldsymbol{I}_M$ and $\boldsymbol{G} \triangleq \boldsymbol{G}_r \in \mathbb{R}^{M \times M}$. ■

Note that the thereom is closely related to the geometry of projection matrices [20].[6] It has been shown that given the initial conditions $\boldsymbol{P}(0) \in \mathcal{P}$ and $(d\boldsymbol{P}(0)/dt)$, a geodesic curve on the manifold of projection matrices $\mathcal{P}$ can be obtained by

$$\boldsymbol{P}(t) = e^{\boldsymbol{A}t}\boldsymbol{P}(0)e^{-\boldsymbol{A}t} \tag{18}$$

where the constant skew-Hermitian matrix

$$\boldsymbol{A} \triangleq \left.\frac{d\boldsymbol{P}(t)}{dt}\right|_0 \boldsymbol{P}(0) - \boldsymbol{P}(0) \left.\frac{d\boldsymbol{P}(t)}{dt}\right|_0 \tag{19}$$

defines the corresponding differential equation

$$\frac{d\boldsymbol{P}(t)}{dt} = \boldsymbol{A}\boldsymbol{P}(t) - \boldsymbol{P}(t)\boldsymbol{A}. \tag{20}$$

[5]Given $\boldsymbol{A} \in \mathbb{C}^{M \times N}$, the 2-norm of $\boldsymbol{A}$ equals $||\boldsymbol{A}||_2 \triangleq \max_{\boldsymbol{x} \neq \boldsymbol{0}} \sqrt{(\boldsymbol{x}^H\boldsymbol{A}^H\boldsymbol{A}\boldsymbol{x})/(\boldsymbol{x}^H\boldsymbol{x})} = \sqrt{\lambda_{\max}(\boldsymbol{A}^H\boldsymbol{A})}$.

[6]A tutorial summary of the key elements of the geometry of the manifold of projection matrices can be found in [21].

According to the optimization problem in (8), where $\boldsymbol{P}$ plays the role of the matrix argument of a given objective function $\tilde{J}(\boldsymbol{P})$, and given the parameterization of $\boldsymbol{P}$ by Lemma 1, an obvious choice for the derivative matrix in (19) is apparently given by

$$\left.\frac{d\boldsymbol{P}(t)}{dt}\right|_0 = -\sum_{i=1}^{M^2} \left.\frac{\partial \boldsymbol{P}(\boldsymbol{\theta})}{\partial \theta_i}\right|_{\boldsymbol{0}} \left.\frac{\partial \tilde{J}(\boldsymbol{\theta})}{\partial \theta_i}\right|_{\boldsymbol{0}} \tag{21}$$

where $\boldsymbol{\theta}$ composes the vectors $\boldsymbol{\phi}, \boldsymbol{\sigma}$, and $\boldsymbol{\xi}$, and θ_i serves as a representative for any one of these parameters, respectively. Accordingly, referring to (19), a candidate skew-Hermitian matrix would be obtained by

$$\boldsymbol{A} = -\sum_{i=1}^{M^2} \left(\left.\frac{\partial \boldsymbol{Q}(\boldsymbol{\theta})}{\partial \theta_i}\right|_{\boldsymbol{0}} \boldsymbol{P}(0) - \boldsymbol{P}(0) \left.\frac{\partial \boldsymbol{Q}^H(\boldsymbol{\theta})}{\partial \theta_i}\right|_{\boldsymbol{0}} \right) \left.\frac{\partial \tilde{J}(\boldsymbol{\theta})}{\partial \theta_i}\right|_{\boldsymbol{0}}. \tag{22}$$

Obviously, the resulting matrix flow $\boldsymbol{P}(t)$ at $t = 0$ would correspond to the gradient of $\tilde{J}(\boldsymbol{P})$. However, although these geometric considerations enlighten the theory of projector tracking substantially, Theorem 2 implies an alternative approach, which is especially relevant from a numerical point of view.

V. Tracking by Incremental Rotations

Theorem 2 ensures the required conditions for any calculus on the manifold of projection matrices $\boldsymbol{P}_u \in \mathbb{C}^{M \times M}$. Let $\mathcal{U}_\epsilon(\boldsymbol{P}_u)$ be an ϵ-ball centered at the projection matrix $\boldsymbol{P}_u$; then, any projection matrix $\boldsymbol{P}_v \in \mathcal{U}_\epsilon(\boldsymbol{P}_u)$ can be approximated by means of a sequence of *real-valued Givens rotations* $\boldsymbol{G}$ and subsequent complex-valued *scaling operations* $\boldsymbol{\Gamma}$ applied to $\boldsymbol{P}_{\mathbf{u}}$. The size of ϵ therefore depends on the required upper bound of the approximation error δ.

Consequently, Theorem 2 implies how to track a projector $\boldsymbol{P}$ while preserving its rank. To this end, we iteratively follow the varying projection matrix by a sequence of projector updates

$$\boldsymbol{P}[t] \leftarrow \boldsymbol{Q}[t] \cdot \boldsymbol{P}[t-1] \cdot \boldsymbol{Q}^H[t] \tag{23}$$

where t again denotes the iteration number, and $\boldsymbol{Q}[t] \triangleq \boldsymbol{\Gamma}[t] \cdot \boldsymbol{G}[t]$. In other words, we follow the varying projection matrix by a sequence of intermediate projection matrices that are connected one by one by overlapping ϵ-balls, respectively.

Behind the update rule in (23), it turns out that we have to run a stochastic gradient approach on the manifold of $\phi_{k,\ell}[t] \in [-\pi, +\pi]$ and $\xi_m[t] \in [-(\pi/2), +(\pi/2)]$, which constitute the manifold of equal-rank projection operators in the ϵ-ball centered arround $\boldsymbol{P}[t-1]$:

$$\Delta\phi_{k,\ell}[t] \leftarrow -\mu \left.\frac{\partial \tilde{J}(\boldsymbol{\theta}[t-1])}{\partial \phi_{k,\ell}}\right|_{\boldsymbol{0}} \tag{24}$$

$$\Delta\xi_m[t] \leftarrow -\mu \left.\frac{\partial \tilde{J}(\boldsymbol{\theta}[t-1])}{\partial \xi_m}\right|_{\boldsymbol{0}}. \tag{25}$$

For the sake of reduced numerical complexity according to the calculation of the partial derivatives, here, we make use of a permanent shift of the initial projection matrix (cf. [23]). Consequently, the algorithm only requires partial derivatives at $\phi_{k,\ell} = 0$ and $\xi_m = 0$. The constant parameter $\mu > 0$ determines

the step size of the steepest-descent optimization method. The choice of μ influences the convergence and accuracy of the iterative algorithm and has been chosen experimentally for the simulation results in Section VII.

A. Complex-Valued Subspaces

In the case of complex-valued signal subspaces, the increments $\Delta\phi_{k,\ell}$ and $\Delta\xi_m$ are due to the gradient of the objective function in (9), where $\boldsymbol{P}$ is replaced by $\boldsymbol{Q}(\boldsymbol{\theta})\boldsymbol{P}\boldsymbol{Q}(\boldsymbol{\theta})$

$$\tilde{J}(\boldsymbol{Q}(\boldsymbol{\theta})) \stackrel{\triangle}{=} \mathrm{tr}(\hat{\boldsymbol{R}}_x) - \mathrm{tr}(\hat{\boldsymbol{R}}_x\boldsymbol{Q}(\boldsymbol{\theta})\boldsymbol{P}\boldsymbol{Q}^H(\boldsymbol{\theta})). \tag{26}$$

Taking into account that $\mathrm{tr}(\hat{\boldsymbol{R}}_x\boldsymbol{P}) \equiv \mathrm{tr}(\boldsymbol{P}\hat{\boldsymbol{R}}_x) \equiv \langle\hat{\boldsymbol{R}}_x, \boldsymbol{P}\rangle \equiv \langle\boldsymbol{P}, \hat{\boldsymbol{R}}_x\rangle$, where, respectively, $\hat{\boldsymbol{R}}_x = \hat{\boldsymbol{R}}_x^H \in \mathbb{C}^{M\times M}$, $\boldsymbol{P} = \boldsymbol{P}^H \in \mathbb{C}^{M\times M}$, and $\langle\bullet,\bullet\rangle$ denotes the inner product of two matrices,[7] the derivatives of $\tilde{J}(\boldsymbol{\theta})$ according to the parameters $\boldsymbol{\theta}$ at $\boldsymbol{\theta} = \boldsymbol{0}$ are equal to

$$\begin{aligned}\left.\frac{\partial\tilde{J}(\boldsymbol{\theta})}{\partial\theta_i}\right|_{\boldsymbol{0}} &= -\left\langle\hat{\boldsymbol{R}}_x, \left.\frac{\partial\boldsymbol{Q}(\boldsymbol{\theta})}{\partial\theta_i}\right|_{\boldsymbol{0}}\boldsymbol{P}\boldsymbol{Q}^H(\boldsymbol{0}) \right.\\ &\qquad \left. + \boldsymbol{Q}(\boldsymbol{0})\boldsymbol{P}\left.\frac{\partial\boldsymbol{Q}^H(\boldsymbol{\theta})}{\partial\theta_i}\right|_{\boldsymbol{0}}\right\rangle \\ &= -\left\langle\hat{\boldsymbol{R}}_x, \left.\frac{\partial\boldsymbol{Q}(\boldsymbol{\theta})}{\partial\theta_i}\right|_{\boldsymbol{0}}\boldsymbol{P} + \boldsymbol{P}\left.\frac{\partial\boldsymbol{Q}^H(\boldsymbol{\theta})}{\partial\theta_i}\right|_{\boldsymbol{0}}\right\rangle \qquad (27)\\ &= -2\mathrm{Re}\left\{\left\langle\hat{\boldsymbol{R}}_x, \left.\frac{\partial\boldsymbol{Q}(\boldsymbol{\theta})}{\partial\theta_i}\right|_{\boldsymbol{0}}\boldsymbol{P}\right\rangle\right\}. \qquad (28)\end{aligned}$$

Referring to Lemma 1, the first-order derivatives of $\tilde{J}(\boldsymbol{\theta})$ at $\boldsymbol{\theta} = \boldsymbol{0}$ according to $\phi_{k,\ell}$ und ξ_m can be written as

$$\begin{aligned}\left.\frac{\partial\tilde{J}}{\partial\phi_{k,\ell}}\right|_0 &= 2\mathrm{Re}\left\{\boldsymbol{P}^{(\ell)}\hat{\boldsymbol{R}}_{x,(k)}\right\} - 2\mathrm{Re}\left\{\boldsymbol{P}^{(k)}\hat{\boldsymbol{R}}_{x,(\ell)}\right\}\\ &= 2\mathrm{Re}\left\{\sum_{i=1}^{M}P_{\ell,i}\hat{R}_{i,k} - P_{k,i}\hat{R}_{i,\ell}\right\} \qquad (29)\\ \left.\frac{\partial\tilde{J}}{\partial\xi_m}\right|_0 &= 2\mathrm{Im}\left\{\boldsymbol{P}^{(m)}\hat{\boldsymbol{R}}_{x,(m)}\right\}\\ &= 2\mathrm{Im}\left\{\sum_{i=1}^{M}P_{m,i}\hat{R}_{i,m}\right\} \qquad (30)\end{aligned}$$

where $\boldsymbol{P}^{(\ell)}$ and $\hat{\boldsymbol{R}}_{x,(k)}$ are the ℓth row vector and the kth column vector of the matrices $\boldsymbol{P}$ and $\hat{\boldsymbol{R}}_x$, respectively, and $P_{k,\ell}$ and $\hat{R}_{k,\ell}$ are the corresponding entries of the matrices $\boldsymbol{P}$ and $\hat{\boldsymbol{R}}_x$.

Hence, the entirely updated projection matrix is given in (31), where the $\Delta\phi_{k,\ell}$ and $\Delta\xi_m$ are obtained according to (24), (25), (29), and (30).

$$\begin{aligned}\boldsymbol{P}[t] = \mathrm{diag}[&e^{j\Delta\xi_1},\ldots,e^{j\Delta\xi_M}]\\ &\times\prod_{k=M-1}^{1}\prod_{\ell=k+1}^{M}\boldsymbol{G}_r^{k,\ell}(\Delta\phi_{k,\ell},0)\boldsymbol{P}[t-1]\prod_{k=1}^{M-1}\\ &\times\prod_{\ell=M}^{k+1}\boldsymbol{G}_r^{k,\ell}(-\Delta\phi_{k,\ell},0)\mathrm{diag}[e^{-\mathrm{j}\Delta\xi_1},\ldots,e^{-j\Delta\xi_M}].\end{aligned} \tag{31}$$

[7] $\langle\boldsymbol{U},\boldsymbol{V}\rangle \equiv \sum_{j=1}^{M}\langle\boldsymbol{u}_j,\boldsymbol{v}_j\rangle \equiv \sum_{j=1}^{M}\boldsymbol{u}_j^H\boldsymbol{v}_j \equiv \sum_{i=1}^{M}\sum_{j=1}^{M}u_{ij}^*v_{ij}$.

Obviously, the update of $\boldsymbol{P}$ in (31) can be efficiently implemented by a sequence of pre- and post-multiplications of $\boldsymbol{P}$ with the rotation matrices $\boldsymbol{G}_r^{k,\ell}(\Delta\phi_{k,\ell},0)$ and $\boldsymbol{G}_r^{k,\ell}(-\Delta\phi_{k,\ell},0)$, respectively.

Referring to (23), (31), and (6), the update of the corresponding basis vectors $\boldsymbol{W}[t] \in \mathbb{C}^{M\times d}$, where $\boldsymbol{P}[0] = \boldsymbol{W}[0]\boldsymbol{W}^H[0]$, can be obtained by

$$\boldsymbol{W}[t] \leftarrow \boldsymbol{\Gamma}(\boldsymbol{\xi})\boldsymbol{G}_r(\boldsymbol{\phi},\boldsymbol{0})\boldsymbol{W}[t-1]. \tag{32}$$

Exploiting the structure of the matrices $\boldsymbol{\Gamma}$ and $\boldsymbol{G}_r^{k,l}$ results in an efficient implementation of the update rule given in Table I.

The subspace projector tracking has been originally developed for blockwise data processing. However, a sequential data processing mode of the proposed method can be given. Therefore, the first-order derivatives now mean

$$\left.\frac{\partial\tilde{J}}{\partial\phi_{k,\ell}}\right|_0 = 2\mathrm{Re}\left\{\sum_{i=1}^{M}P_{\ell,i}x_ix_k^* - P_{k,i}x_ix_\ell^*\right\} \tag{33}$$

$$\left.\frac{\partial\tilde{J}}{\partial\xi_m}\right|_0 = 2\mathrm{Im}\left\{\sum_{i=1}^{M}P_{m,i}x_ix_m^*\right\}. \tag{34}$$

B. Real-Valued Subspaces

If the matrix of eigenvectors corresponding to dominant eigenvalues $\boldsymbol{U}_s$ and the projection matrix $\boldsymbol{P}$ are elements of $\mathbb{R}^{M\times d}$ and $\mathbb{R}^{M\times M}$, the first-order derivatives of $\tilde{J}(\boldsymbol{\theta})$ at $\boldsymbol{\theta} = \boldsymbol{0}$ according to $\phi_{k,\ell}$ and ξ_m simplify to

$$\left.\frac{\partial\tilde{J}}{\partial\phi_{k,\ell}}\right|_0 = 2\left(\sum_{i=1}^{M}P_{\ell,i}\hat{R}_{i,k} - P_{k,i}\hat{R}_{i,\ell}\right) \tag{35}$$

$$\left.\frac{\partial\tilde{J}}{\partial\xi_m}\right|_0 = 2\left(\sum_{i=1}^{M}P_{m,i}\hat{R}_{i,m}\right). \tag{36}$$

VI. Numerical Complexity

The implementation of (32) according to Table I requires $2MNd+2M^2d$ complex-valued multiplications, where the numerical effort in number of multiplications is summarized according to

$$\begin{aligned}\boldsymbol{\Upsilon}[t]&: \ 2MNd\\ \Delta\boldsymbol{\phi}&: \ M(M-1)d\\ \Delta\boldsymbol{\xi}&: \ Md\\ \boldsymbol{W}[t]&: \ M(M-1)d + Md.\end{aligned}$$

On the other hand, the update rule of $\boldsymbol{W}$ according to (6) requires $3MNd$ complex-valued multiplications. This means that in the blockwise processing mode, the subspace projector tracking algorithm becomes more efficient if the size N of the data blocks grows (cf. Section VII, Table II). Since the numerical complexity increases quadratically with the number of antenna elements, the proposed method seems to be most interesting for small-sized antenna configurations (cf. Section VII, Table I).

In the case of sequential processing instead of blockwise processing, the projector based tracking exhibits a complexity of $\mathcal{O}(M^2d)$, whereas the complexity of the PAST algorithm is equal to $\mathcal{O}(Md)$.

TABLE I
UPDATE RULE $\boldsymbol{W}[t] \leftarrow \boldsymbol{\Gamma}\boldsymbol{G}_r\boldsymbol{W}[t-1]$. $W_{\ell,i}$ AND $\Upsilon_{i,k}$ ARE THE CORRESPONDING ENTRIES OF THE MATRICES $\boldsymbol{W}[t-1]$ AND $\boldsymbol{\Upsilon}[t]$. THE VECTOR $\boldsymbol{W}^{(m)}$ DENOTES THE m-TH ROW VECTOR OF $\boldsymbol{W}$

$\boldsymbol{Y}[t] \leftarrow \boldsymbol{W}^{\mathrm{H}}[t-1]\boldsymbol{X}[t]$

$\boldsymbol{\Upsilon}[t] \leftarrow \boldsymbol{Y}[t]\boldsymbol{X}^{\mathrm{H}}[t]$

`for` $k = 1, 2, \ldots, M-1$ (`real-valued` *Givens rotations*)

  `for` $\ell = M, M-1, \ldots, k+1$

    $\phi_{k,\ell} \leftarrow -2\mu\mathrm{Re}\left\{\sum_{i=1}^{d} W_{\ell,i}\Upsilon_{i,k} - W_{k,i}\Upsilon_{i,\ell}\right\}$

    $c_{k,l} \leftarrow \cos(\phi_{k,l})$, $s_{k,l} \leftarrow \sin(\phi_{k,l})$

    $$\begin{bmatrix} \boldsymbol{W}^{(k)}[t] \\ \boldsymbol{W}^{(\ell)}[t] \end{bmatrix} \leftarrow \begin{bmatrix} c_{k,l} & -s_{k,l} \\ s_{k,l} & c_{k,l} \end{bmatrix} \begin{bmatrix} \boldsymbol{W}^{(k)}[t-1] \\ \boldsymbol{W}^{(\ell)}[t-1] \end{bmatrix}$$

  `end`

`end`

`for` $m = 1, 2, \ldots, M$ (`complex-valued` *scaling operations*)

  $\xi_m \leftarrow -2\mu\mathrm{Im}\left\{\sum_{i=1}^{d} W_{m,i}\Upsilon_{i,m}\right\}$

  $\gamma_m \leftarrow \exp(\mathrm{j}\xi_m)$

  $\boldsymbol{W}^{(m)}[t] \leftarrow \gamma_m \boldsymbol{W}^{(m)}[t-1]$

`end`

TABLE II
COMPUTATIONAL COMPLEXITY OF THE REAL-VALUED SIGNAL SUBSPACE ESTIMATION SCHEMES

Est. scheme	real add.	real mult.
Calc. of $\hat{\boldsymbol{R}}_{\mathbf{x}}$	$(2N-1)\frac{M(M+1)}{2}$	$NM(M+1)$
Mod. Jacobi	$\mathcal{O}(M^3)$	$\mathcal{O}(M^3)$
PAST	$6MNd$	$6MNd$
Proj. tracking	$3M^2(M-1)$	$3M^2(M-1)$

Finally, the rotation-type nature of the subspace projector tracking initiates alternative solutions for the VLSI implementation of the tracking algorithm, e.g., cordinate rotation digital computer (CORDIC)-based techniques. The basic idea of the CORDIC scheme is to map the elementary *Givens rotation* angles $\phi_{k,\ell}$ to a binary sequence representing powers of two. According to this sequence, each elementary *Givens rotation* is performed by a sequence of CORDIC rotations with their rotation angles being powers of two [22]. Let assume a two-dimensional (2-D) *Givens rotation* by angle ϕ

$$\begin{bmatrix} c & -s \\ s & c \end{bmatrix} = c \cdot \begin{bmatrix} 1 & -t \\ t & 1 \end{bmatrix} \tag{37}$$

where $c \triangleq \cos(\phi), s \triangleq \sin(\phi)$, and $t \triangleq \tan(\phi)$. Then, the rotation matrix is denoted by a sequence of elementary rotations with angle ϕ_i. If the ϕ_i are chosen such that $\phi_i = \pm\arctan(2^{-i})$, they can be realized by simple shifts and additions. With $\cos(\arctan(2^{-i})) = (1)/(\sqrt{1+2^{-2i}})$, the original rotation matrix can be written as

$$\prod_{i=0}^{\infty} \frac{1}{\sqrt{1+2^{-2i}}} \begin{bmatrix} 1 & \mp 2^{-i} \\ \pm 2^{-i} & 1 \end{bmatrix}. \tag{38}$$

This is very suitable for a hardware implementation of the scheme, as multiplications are avoided. In practice, the series of CORDIC rotations is stopped after L rotations. Note that after each CORDIC rotation, a rescaling with the factor $(1)/(\sqrt{1+2^{-2i}})$ has to be done. However, it was shown that this rescaling operation can also be replaced by means of shift-add operations.

VII. SIMULATION RESULTS ON DOA TRACKING

The performance evaluation of the proposed algorithm is based on the DOA estimation by means of ESPRIT [3]. Therefore, the signal subspace estimation has been of particular interest since this step of ESPRIT-like methods generally turns out to be the most time-consuming part. In order to get close to real systems, a DSP served as the hardware processor. Implementation is done on the C6701 32-bit floating point DSP from Texas Instruments with a clock rate of 150 MHz [23]. The supported very long instruction word technique (VLIW) enables the DSP to address its multiple hardware units simultaneously and to carry out up to eight instructions per clock cycle. The source code is completely written in `C` and represents an implementation of the 2-D-Unitary ESPRIT [24]. Thus, two parameters of each of the impinging wavefronts at a uniform rectangular antenna array (URA) can be resolved: the azimuth angles φ_i and the elevation angles ϑ_i of the DOAs.

Since the DSP is not part of a real system, the input data of 2-D-Unitary ESPRIT is generated by MATLAB. Therefore, the transmission medium is assumed to be isotropic and linear. The noise is modeled as a complex, zero-mean white Gaussian process. Under the assumptions of narrowband and farfield signals, the complex baseband measurements of the kth antenna element can be described as

$$x_k = \sum_{i=1}^{d} \rho_k \cdot s_i \cdot e^{-j\frac{2\pi}{\lambda_c}\langle \vec{e}(\varphi_i,\vartheta_i),\vec{r}_k\rangle} + n_k \tag{39}$$

$1 \le k \le M$, where the (φ_i, ϑ_i) refer to the DOA parameters of the ith wavefront, and $\vec{e}(\varphi_i, \vartheta_i)$ and $\vec{r}_k$ denote the unit vector steering in direction of (φ_i, ϑ_i) and the coordinate vector of the kth antenna element within the array of size M. The n_k is the additive white Gaussian noise, and ρ_k is the complex response of the kth sensor element. The d indicates the number of impinging wavefronts. The s_i are the complex envelopes of the impinging signals, which are BPSK-modulated with no oversampling. Calculating the x_k for all M sensor elements and collecting the data over N snapshots yields the data matrix $\boldsymbol{X}$ serving as input for 2-D-Unitary ESPRIT.

Two-dimensional Unitary ESPRIT itself can be divided into three major steps [24]. First, the real-valued signal subspace is estimated. Subsequently, two independent invariance equations are formed and solved. Finally, the eigenvalues of the solution matrices of the second step lead to the desired DOA parameters.

Three signal subspace estimation schemes are subject to the following performance comparison: the modified Jacobi method [16], [25], PAST [6], and the projector tracking. In order to save runtime, the Jacobi method has been modified [26]. The basic idea is to concentrate the data relevant for the

TABLE III
SCENARIO FOR COMPARING THE SIGNAL SUBSPACE ESTIMATION SCHEMES

Scenario
URA with $M = 3 \times 3 \ldots 5 \times 5$
$N = 20 \ldots 160$ snapshots / slot
$d = 3$ impinging wavefronts
100 slots
10 averaging trials
change of the azimuth/elevation angle from slot to slot: 0.1°
from (initial slot): $\vartheta = [15°\ \ 40°\ \ 75°]\ \ \varphi = [-40°\ \ 0°\ \ 40°]$
to (last slot): $\vartheta = [25°\ \ 50°\ \ 65°]\ \ \varphi = [-30°\ \ -10°\ \ 50°]$
BPSK modulation and additive white Gaussian noise (AWGN)
SNR $= -5 \ldots 30$ dB

signal subspace in a preprocessing step (Hessenberg transform [16]) and then perform the Jacobi method with a smaller matrix.

For the startup of the algorithm, the number of impinging wavefronts is required. Since subspace projector tracking is a rank-preserving algorithm, it obviously depends on the *a priori* knowledge of the system order [27], [28]. The initial value of $\boldsymbol{P}$ is set to the matrix that contains ones at the first d diagonal elements and zeros elsewhere.

In Table III, the scenario used for performance evaluation is presented. It is evident that the signal subspace estimation is the most time-consuming part, especially when large URAs are used. In the following, the results of the execution time comparison of the three signal subspace estimation methods based on blockwise data processing are presented.[8] Table II lists an assessment of the computational complexity of the schemes subject to M, N, and d. Note that PAST directly operates on the real-valued data matrix, whereas the two other methods need the estimation of the covariance matrix $\hat{\boldsymbol{R}}_x$. Therefore, the number of calculations needed for the computation of $\hat{\boldsymbol{R}}_x$ has to be added to the execution times of Jacobi and projector tracking in order to get comparable results. Moreover, note that the projector tracking directly operates on the projection matrix [cf. (31)] instead of following the algorithm in Table I.

Figs. 1 and 2 illustrate the results of DSP simulations. Execution times of the subspace estimation subject to M are shown in Fig. 1 and subject to N in Fig. 2, respectively. As can be seen easily, the tracking schemes are able to reduce the computation time of the signal subspace significantly compared with the modified Jacobi method. With respect to each other, either PAST or projector tracking achieves a better performance, depending on the number of antenna elements and snapshots, respectively. The PAST algorithm shows a better computation rate for small N and large M, whereas projector tracking achieves a better result for large N and small M. This is due to the different dependencies of the computational complexity on the parameters M and N, cf. Section VI and Table II for the complex-valued mode and the real-valued case, respectively.

With respect to the accuracy of the estimated DOAs, the RMS has been taken as a measure of accuracy. It reads

$$\text{RMS} = \sqrt{\frac{1}{n}\sum \left\| \begin{bmatrix} \vartheta_{\text{est}} \\ \varphi_{\text{est}} \end{bmatrix} - \begin{bmatrix} \vartheta \\ \varphi \end{bmatrix} \right\|^2} \tag{40}$$

[8]Note that applying 2-D-Unitary ESPRIT determines the sample covariance matrix $\hat{\boldsymbol{R}}_x$ to be real-valued.

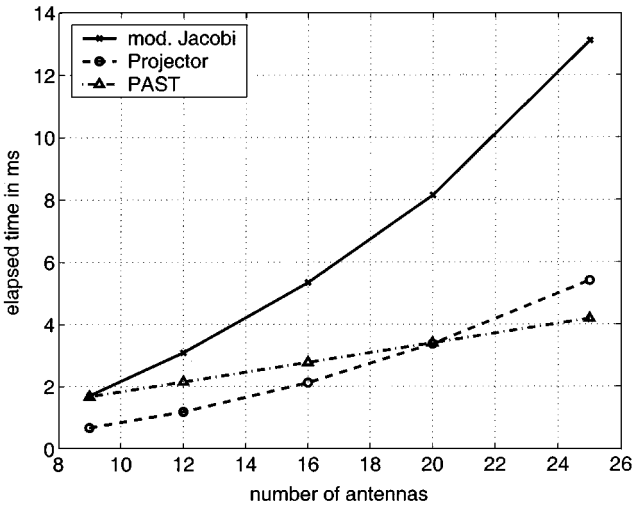

Fig. 1. Execution time of the modified Jacobi method, PAST, and projector tracking, depending on the number of antennas M: $N = 140$ snapshots.

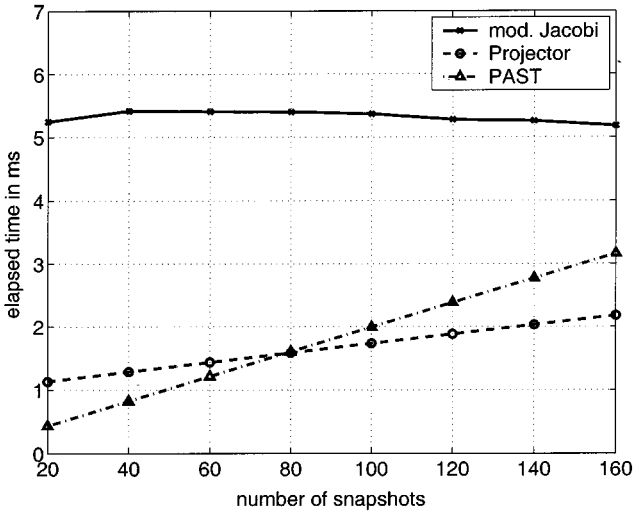

Fig. 2. Execution time of the modified Jacobi method, PAST, and projector tracking, depending on the number of snapshots N: $M = 4 \times 4$ antenna elements.

where n denotes the number of averaging trials. The $\vartheta_{\text{est}}, \varphi_{\text{est}}, \vartheta$, and φ are the estimated and the actual vectors of angles of the instantaneous DOAs, respectively. Compared with subspace estimation by means of the modified Jacobi method, where playing with a forgetting factor to estimate the covariance matrix has been included, both tracking schemes achieve more accurate results in scenarios with low SNRs Fig. 3. Therefore, the step-size $\mu > 0$ of both tracking methods have been chosen carefully between 0.001 and 0.01. Note that the tracking accuracy decreases in scenarios with rapid changes of the DOAs from slot to slot. The modified Jacobi method outperforms the projector tracking at high SNR values and in scenarios of rapidly changing DOAs ($\uparrow$ DOA/slot), where the tracking algorithm suffers from a degraded convergence capability Fig. 4.

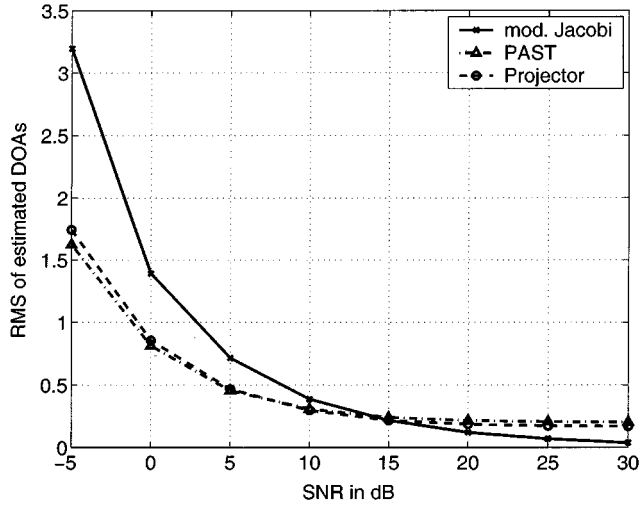

Fig. 3. RMS comparison of modified Jacobi EVD, projector tracking, and PAST: $M = 4 \times 4$ antenna elements and $N = 140$ snapshots.

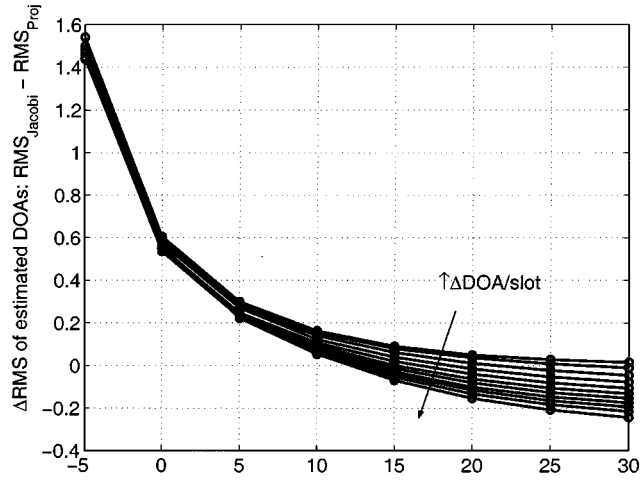

Fig. 4. RMS comparison of modified Jacobi and projector tracking for changing DOAs:$\{\Delta\text{azimuth}, \Delta\text{elevation}\} \cdot \text{slot}^{-1} = \{0.0^\circ, \ldots, 2.0^\circ\} \cdot \text{slot}^{-1}$, $M = 4 \times 4$ antenna elements, and $N = 140$ snapshots.

VIII. Conclusion

Whereas the tracking of the unitary basis of signal subspaces has been the subject of a number of publications in the past, the immediate tracking of the unique projection matrix of the signal subspace was first proposed in [20], [29], and [30]. There, the authors presented an approach to subspace tracking either based on geodesic trajectories on the manifold of projection matrices [20], [21] or closely related by means of gradient flows that requires permanent computation of the exponential of $M \times M$ skew-Hermitian matrices [29], [30]. In this work, a different parameterization of the local manifold of given projection matrices has been proposed. To this end, projection matrices are parameterized by means of incremental *Givens rotations* followed by subsequent *scaling operations*.

In numerical experiments, by means of DSP implementations, it turns out that the estimation accuracy of the subspace projector tracking is rather comparable with the PAST algorithm. In terms of the required numerical complexity, the projector tracking algorithm outperforms the PAST algorithm, especially for small-sized antenna configurations and block-wise data processing about a factor of $\approx 1.5 \cdots 2$ (see Tables I and II). However, for the sequential data processing mode, the PAST-like algorithms outperform the numerical complexity of projector tracking by an order of magnitude Section VI.

Furthermore, the subspace projector tracking algorithm offers two important advantages. First, in contrast to `matrix×vector` operation-based algorithms (PAST, etc.), the rotation-type nature of the projector tracking allows alternative VLSI realizations of the algorithm based on CORDIC-like techniques, which would let the projector tracking algorithm surpass PAST-like algorithms, even in sequential data processing applications. Second, the proposed new parameterization of projection matrices offers an alternative solution to encode moderate changes of subspaces by a minimum of parameters, i.e., $(M(M+1))/(2)$ instead of $2Md$ parameters. This has become exceptionally important in closed-loop Tx-diversity downlink concepts in UMTS Wideband CDMA, where the number of antenna elements is rather low [31], [32].

Appendix A
Derivatives of $\mathbf{Q}$

The first and second-order derivatives of $\boldsymbol{Q}$ with respect to $\phi_{k,\ell}, \sigma_{k,\ell}$, and ξ_m, i.e., according to the parameterization of unitary matrices given by Lemma 1, can be denoted as follows. Here, the $(\partial/\partial\phi_{k,\ell})|_{\left[\begin{smallmatrix}k,k & k,\ell\\ \ell,k & \ell,\ell\end{smallmatrix}\right]}$ and $(\partial/\partial\xi_m)|_{[k,k]}$ denote the non-vanishing characteristic 2×2 submatrix or the addressed element of the respective derivatives of $\boldsymbol{Q}$, when any other elements of the matrix are equal to zero. Note that the derivatives are always taken at $\phi_{k,\ell} = 0, \sigma_{k,\ell} = 0$, and $\xi_m = 0$.

$$\left.\frac{\partial \boldsymbol{G}}{\partial \phi_{k,\ell}}\right|_{\left[\begin{smallmatrix}k,k & k,\ell\\ \ell,k & \ell,\ell\end{smallmatrix}\right]} = \begin{bmatrix} 0 & -1 \\ 1 & 0 \end{bmatrix} \tag{41}$$

$$\frac{\partial \boldsymbol{G}}{\partial \sigma_{k,\ell}} = \mathbf{0} \tag{42}$$

$$\left.\frac{\partial \boldsymbol{\Gamma}}{\partial \xi_m}\right|_{[k,k]} = j \tag{43}$$

$$\left.\frac{\partial^2 \boldsymbol{G}}{\partial \phi_{k,\ell}^2}\right|_{\left[\begin{smallmatrix}k,k & k,\ell\\ \ell,k & \ell,\ell\end{smallmatrix}\right]} = \begin{bmatrix} -1 & 0 \\ 0 & -1 \end{bmatrix} \tag{44}$$

$$\frac{\partial^2 \boldsymbol{G}}{\partial \sigma_{k,\ell}^2} = \mathbf{0} \tag{45}$$

$$\left.\frac{\partial^2 \boldsymbol{\Gamma}}{\partial \xi_m^2}\right|_{[k,k]} = -1 \tag{46}$$

respectively, and[9]

$$\frac{\partial^2 \boldsymbol{G}}{\partial \phi_{k,\ell} \partial \phi_{p,q}} = \frac{\partial^2 \boldsymbol{G}}{\partial \phi_{p,q} \partial \phi_{k,\ell}} = \begin{cases} \frac{\partial G}{\partial \phi_{k,\ell}} \frac{\partial G}{\partial \phi_{p,q}}, & \{k > p\} \quad \vee \quad \{k = p \quad \wedge \quad l < q\} \\ \frac{\partial G}{\partial \phi_{p,q}} \frac{\partial G}{\partial \phi_{k,\ell}}, & \{k < p\} \quad \vee \quad \{k = p \quad \wedge \quad l > q\} \end{cases} \tag{47}$$

$$\frac{\partial^2 \boldsymbol{G}}{\partial \phi_{k,\ell} \partial \sigma_{k,\ell}} = \frac{\partial^2 \boldsymbol{G}}{\partial \sigma_{k,\ell} \partial \phi_{k,\ell}} = \mathbf{0} \tag{48}$$

[9]For the derivation of (47), the order of appearance of the matrices $\boldsymbol{G}^{k,\ell}$ in (12) plays an important role.

$$\frac{\partial^2 \boldsymbol{Q}}{\partial\phi_{k,\ell}\partial\xi_m} = \frac{\partial^2 \boldsymbol{Q}}{\partial\xi_m\partial\phi_{k,\ell}} = \frac{\partial\boldsymbol{\Gamma}}{\partial\xi_m}\frac{\partial\boldsymbol{G}}{\partial\phi_{k,\ell}} \tag{49}$$

$$\frac{\partial^2 \boldsymbol{G}}{\partial\sigma_{k,\ell}\partial\sigma_{p,q}} = \boldsymbol{0} \tag{50}$$

$$\frac{\partial^2 \boldsymbol{Q}}{\partial\sigma_{k,\ell}\partial\xi_m} = \frac{\partial^2 \boldsymbol{Q}}{\partial\xi_m\partial\sigma_{k,\ell}} = \boldsymbol{0} \tag{51}$$

$$\left.\frac{\partial^2\boldsymbol{\Gamma}}{\partial\xi_m\partial\xi_n}\right|_{m\neq n} = \boldsymbol{0}. \tag{52}$$

It can be easily verified that the 2-norm of the first-order derivative matrices at any $\phi_{k,\ell}, \sigma_{k,\ell}$, and ξ_m is equal to 0 and 1, respectively. Thus, the 2-norm of any first and second-order derivative matrix is upper bounded by

$$\left\|\frac{\partial \boldsymbol{Q}}{\partial\theta_i}\right\|_2 \leq 1 \tag{53}$$

and

$$\left\|\frac{\partial^2 \boldsymbol{Q}}{\partial\theta_i\partial\theta_j}\right\|_2 \leq \left\|\frac{\partial \boldsymbol{Q}}{\partial\theta_i}\right\|_2 \left\|\frac{\partial \boldsymbol{Q}}{\partial\theta_j}\right\|_2 \leq 1 \tag{54}$$

where θ_i and θ_j act in place of $\phi_{k,\ell}, \sigma_{k,\ell}$, and ξ_m.

Finally, in the case of $\phi_{k,\ell} \neq 0, \sigma_{k,\ell} \neq 0$, and $\xi_m \neq 0$, we only refer to the upper bounded 2-norms of the first and second-order derivatives, which, again, are equal to the bounds in (53) and (54). In both cases, the derivation of the bounds benefits from the fact that both the first and the second derivative matrices of $\boldsymbol{Q}$ remain unitary matrices, i.e.,

$$\frac{\partial \boldsymbol{Q}^H}{\partial\theta_i}\frac{\partial \boldsymbol{Q}}{\partial\theta_i} = \boldsymbol{I}_M$$

$$\frac{\partial^2 \boldsymbol{Q}^H}{\partial\theta_i\partial\theta_j}\frac{\partial^2 \boldsymbol{Q}}{\partial\theta_i\partial\theta_j} = \boldsymbol{I}_M.$$

Appendix B
Proof of Theorem 2

1) Given two unitary matrices $\boldsymbol{U}, \boldsymbol{V} \in \mathbb{C}^{M\times d}$ and $\boldsymbol{V} = \boldsymbol{Q}\boldsymbol{U}$, the matrix $\boldsymbol{Q} = \mathbb{C}^{M\times M}$ is also a unitary matrix. Thus, according to the Lemma 1, $\boldsymbol{V}$ is equal to

$$\boldsymbol{V} = \boldsymbol{Q}\boldsymbol{U} = \boldsymbol{\Gamma}\left(\prod_{k=M-1}^{1}\prod_{\ell=k+1}^{M}\boldsymbol{G}^{k,\ell}\right)\boldsymbol{U} \tag{55}$$

and $\boldsymbol{V}$ can be written as a function of the parameters $\boldsymbol{\theta}$ with

$$\boldsymbol{V}(\boldsymbol{\theta}) = \boldsymbol{Q}(\boldsymbol{\theta})\boldsymbol{U} = \boldsymbol{I}_M\boldsymbol{U} = \boldsymbol{U} \tag{56}$$

if $\boldsymbol{\theta} = \boldsymbol{0}$. Therefore, $\boldsymbol{\theta} \triangleq [\boldsymbol{\phi}^T, \boldsymbol{\sigma}^T, \boldsymbol{\xi}^T]^T$ composes the vector of the M^2 parameters $[\ldots, \phi_{k,\ell}, \ldots, \sigma_{k,\ell}, \ldots, \xi_m, \ldots]^T$, and θ_i serves as a representative for any one of these parameters, respectively.

2) Referring to (6), we denote two rank d projection matrices $\boldsymbol{P}_u$ and $\boldsymbol{P}_v$ as

$$\boldsymbol{P}_u = \boldsymbol{U}\boldsymbol{U}^H \tag{57}$$

$$\boldsymbol{P}_v = \boldsymbol{V}\boldsymbol{V}^H = \boldsymbol{Q}(\boldsymbol{\theta})\boldsymbol{P}_u\boldsymbol{Q}^H(\boldsymbol{\theta}) \tag{58}$$

respectively.

3) For small perturbations $\boldsymbol{\theta}$ from $\boldsymbol{0}$ and $\nu \in]0, 1[$, the matrix $\boldsymbol{P}_v(\boldsymbol{\theta})$ can be linearly approximated by

$$\boldsymbol{P}_v(\boldsymbol{\theta}) = \tilde{\boldsymbol{P}}_v(\boldsymbol{\theta}) + \boldsymbol{R}(\nu\boldsymbol{\theta}) \tag{59}$$

where

$$\tilde{\boldsymbol{P}}_v(\boldsymbol{\theta}) = \boldsymbol{P}_u + \sum_{i=1}^{M^2}\left(\left.\frac{\partial\boldsymbol{Q}(\boldsymbol{\theta})}{\partial\theta_i}\right|_{\boldsymbol{0}}\boldsymbol{P}_u + \boldsymbol{P}_u\left.\frac{\partial\boldsymbol{Q}^H(\boldsymbol{\theta})}{\partial\theta_i}\right|_{\boldsymbol{0}}\right)\theta_i \tag{60}$$

and $\theta_i = \phi_{k,\ell}, \sigma_{k,\ell}$, and ξ_m, respectively. Referring to the results in Appendix A and the residual term $\boldsymbol{R}(\nu\boldsymbol{\theta})$ of the Taylor series

$$\begin{aligned}\boldsymbol{R}(\nu\boldsymbol{\theta}) = \sum_{i=1}^{M^2}\sum_{j=1}^{M^2}\frac{1}{2}\Bigg(&\left.\frac{\partial^2\boldsymbol{Q}(\boldsymbol{\theta})}{\partial\theta_i\partial\theta_j}\right|_{\nu\boldsymbol{\theta}}\boldsymbol{P}_u \\ &+ \left.\frac{\partial\boldsymbol{Q}(\boldsymbol{\theta})}{\partial\theta_i}\right|_{\nu\boldsymbol{\theta}}\boldsymbol{P}_u\left.\frac{\partial\boldsymbol{Q}^H(\boldsymbol{\theta})}{\partial\theta_j}\right|_{\nu\boldsymbol{\theta}} \\ &+ \boldsymbol{P}_u\left.\frac{\partial^2\boldsymbol{Q}^H(\boldsymbol{\theta})}{\partial\theta_i\partial\theta_j}\right|_{\nu\boldsymbol{\theta}}\Bigg)\theta_i\theta_j\end{aligned} \tag{61}$$

where referring to (59) and applying the results in Appendix A, i.e., (53) and (54), we obtain

$$\begin{aligned}||\boldsymbol{R}(\nu\boldsymbol{\theta})||_2 &= ||\boldsymbol{P}_v(\boldsymbol{\theta}) - \tilde{\boldsymbol{P}}_v(\boldsymbol{\theta})||_2 \\ &\leq \frac{1}{2}||\boldsymbol{P}_u||_2\sum_{i=1}^{M^2}\sum_{j=1}^{M^2}\left(\left\|\left.\frac{\partial^2\boldsymbol{Q}(\boldsymbol{\theta})}{\partial\theta_i\partial\theta_j}\right|_{\nu\boldsymbol{\theta}}\right\|_2\right. &(62)\\ &\quad + 2\left\|\left.\frac{\partial\boldsymbol{Q}(\boldsymbol{\theta})}{\partial\theta_i}\right|_{\lambda\theta_i}\right\|_2\left\|\left.\frac{\partial\boldsymbol{Q}(\boldsymbol{\theta})}{\partial\theta_j}\right|_{\lambda\theta_j}\right\|_2 &(63)\\ &\quad \left.+\left\|\left.\frac{\partial^2\boldsymbol{Q}^H(\boldsymbol{\theta})}{\partial\theta_i\partial\theta_j}\right|_{\nu\boldsymbol{\theta}}\right\|_2\right)|\theta_i||\theta_j| \\ &\leq 2||\boldsymbol{P}_u||_2||\boldsymbol{\theta}||_1^2 &(64)\end{aligned}$$

where $||\boldsymbol{\theta}||_1$ denotes the ℓ^1-norm of $\boldsymbol{\theta}$, and referring to (59) and (60)

$$\begin{aligned}&||\boldsymbol{P}_v(\boldsymbol{\theta}) - \boldsymbol{P}_u||_2 \\ &\quad = ||\tilde{\boldsymbol{P}}_v(\boldsymbol{\theta}) + \boldsymbol{R}(\nu\boldsymbol{\theta}) - \boldsymbol{P}_u||_2 \\ &\quad \leq ||\tilde{\boldsymbol{P}}_v(\boldsymbol{\theta}) - \boldsymbol{P}_u||_2 + ||\boldsymbol{R}(\nu\boldsymbol{\theta})||_2 \\ &\quad \leq \sum_{i=1}^{M^2}\left\|\left(\left.\frac{\partial\boldsymbol{Q}(\boldsymbol{\theta})}{\partial\theta_i}\right|_{\boldsymbol{0}}\boldsymbol{P}_u + \boldsymbol{P}_u\left.\frac{\partial\boldsymbol{Q}^H(\boldsymbol{\theta})}{\partial\theta_i}\right|_{\boldsymbol{0}}\right)\right\|_2|\theta_i| \\ &\qquad + ||\boldsymbol{R}(\nu\boldsymbol{\theta})||_2 \\ &\quad \leq 2||\boldsymbol{P}_u||_2||\boldsymbol{\theta}||_1 + 2||\boldsymbol{P}_u||_2||\boldsymbol{\theta}||_1^2.\end{aligned} \tag{65}$$

4) Since the derivatives of $\boldsymbol{P}_v(\boldsymbol{\theta})$ according to the parameters $\sigma_{k,\ell}$ at $\boldsymbol{\theta} = \boldsymbol{0}$ are equal to the zero matrix,[10] the equality $\tilde{\boldsymbol{P}}_v(\boldsymbol{\theta}) = \tilde{\boldsymbol{P}}_v(\tilde{\boldsymbol{\theta}})$ holds for any $\tilde{\boldsymbol{\theta}}$, where

$$\tilde{\theta}_i = \begin{cases}0, & \theta_i = \sigma_{k,\ell} \\ \theta_i, & \text{otherwise}\end{cases} \quad \text{and} \quad ||\tilde{\boldsymbol{\theta}}||_2 \leq ||\boldsymbol{\theta}||_2. \tag{66}$$

[10]See Appendix A.

Referring to (64), we again obtain

$$\begin{aligned}&||\boldsymbol{P}_v(\tilde{\boldsymbol{\theta}})-\tilde{\boldsymbol{P}}_v(\tilde{\boldsymbol{\theta}})||_2\\&\quad=||\boldsymbol{P}_v(\tilde{\boldsymbol{\theta}})-\tilde{\boldsymbol{P}}_v(\boldsymbol{\theta})||_2\\&\quad\le 2||\boldsymbol{P}_u||_2||\tilde{\boldsymbol{\theta}}||_1^2\\&\quad\le 2||\boldsymbol{P}_u||_2||\boldsymbol{\theta}||_1^2.\end{aligned}\tag{67}$$

Thus, from (64) and (67) it follows that

$$\begin{aligned}&||\boldsymbol{P}_v(\boldsymbol{\theta})-\boldsymbol{P}_v(\tilde{\boldsymbol{\theta}})||_2\\&\quad\le||\boldsymbol{P}_v(\boldsymbol{\theta})-\tilde{\boldsymbol{P}}_v(\boldsymbol{\theta})+\tilde{\boldsymbol{P}}_v(\boldsymbol{\theta})-\boldsymbol{P}_v(\tilde{\boldsymbol{\theta}})||_2\\&\quad\le||\boldsymbol{P}_v(\boldsymbol{\theta})-\tilde{\boldsymbol{P}}_v(\boldsymbol{\theta})||_2+||\tilde{\boldsymbol{P}}_v(\boldsymbol{\theta})-\boldsymbol{P}_v(\tilde{\boldsymbol{\theta}})||_2\\&\quad\le 4||\boldsymbol{P}_u||_2||\boldsymbol{\theta}||_1^2.\end{aligned}\tag{68}$$

Alternatively, the matrix $\boldsymbol{P}_v(\tilde{\boldsymbol{\theta}})$ can be parameterized by (55), where now, the basic unitary matrices $\boldsymbol{G}^{k,\ell}$, and therefore, $\boldsymbol{G}_r$, are real-valued matrices since $\tilde{\sigma}_{k,\ell}=0$ by definition of $\tilde{\boldsymbol{\theta}}$.

5) In the following, we identify the obtained results with expressions in Theorem 2. To this end, (65) is related to (16)

$$||\boldsymbol{P}_v(\boldsymbol{\theta})-\boldsymbol{P}_u||_2\le\epsilon\tag{69}$$

i.e., $\boldsymbol{P}_v(\boldsymbol{\theta})$ lies in the ϵ-ball centered around $\boldsymbol{P}_u$.

We further identify the result in (68) with expression (14). Note that $\boldsymbol{P}_v(\tilde{\boldsymbol{\theta}})=\boldsymbol{Q}(\tilde{\boldsymbol{\theta}})\boldsymbol{P}_u\boldsymbol{Q}^H(\tilde{\boldsymbol{\theta}})$, where $\boldsymbol{Q}(\tilde{\boldsymbol{\theta}})\stackrel{\triangle}{=}\boldsymbol{\Gamma}\cdot\boldsymbol{G}$ and $\boldsymbol{G}=\boldsymbol{G}_r\in\mathbb{R}^{M\times M}$ since $\tilde{\sigma}_{k,\ell}=0$. On the other hand, $||\boldsymbol{P}_v(\boldsymbol{\theta})-\boldsymbol{P}_v(\tilde{\boldsymbol{\theta}})||_2$ is upper bounded by

$$||\boldsymbol{P}_v(\boldsymbol{\theta})-\boldsymbol{\Gamma}(\tilde{\boldsymbol{\theta}})\boldsymbol{G}_r(\tilde{\boldsymbol{\theta}})\boldsymbol{P}_u\boldsymbol{G}_r^T(\tilde{\boldsymbol{\theta}})\boldsymbol{\Gamma}^H(\tilde{\boldsymbol{\theta}})||_2\le\delta.\tag{70}$$

Thus, taking into account the results denoted in (65) and (68), we conclude that

$$\begin{aligned}\delta&=4||\boldsymbol{P}_u||_2||\boldsymbol{\theta}||_1^2\\\epsilon&=2||\boldsymbol{P}_u||_2||\boldsymbol{\theta}||_1+2||\boldsymbol{P}_u||_2||\boldsymbol{\theta}||_1^2.\end{aligned}$$

Finally, we end up with

$$\epsilon=\sqrt{\delta||\boldsymbol{P}_u||_2}+\frac{\delta}{2}=\sqrt{\delta}+\frac{\delta}{2}\tag{71}$$

where we have taken into account that the 2-norm of any projection matrices is equal to 1.

In other words, for each required *precision* $||\boldsymbol{P}_v(\boldsymbol{\theta})-\boldsymbol{\Gamma}(\tilde{\boldsymbol{\theta}})\boldsymbol{G}_r(\tilde{\boldsymbol{\theta}})\boldsymbol{P}_u\boldsymbol{G}_r^T(\tilde{\boldsymbol{\theta}})\boldsymbol{\Gamma}^H(\tilde{\boldsymbol{\theta}})||_2\le\delta$, there *exists* an ϵ-ball centered around $\boldsymbol{P}_u$ such that for all $\boldsymbol{P}_v$ elements of this ball, we can guarantee the requirements.

This concludes the proof. ■

ACKNOWLEDGMENT

The author would like to thank Prof. Dr.-techn. J. A. Nossek, Institute for Circuit Theory and Signal Processing, Technische Universität München, for his generous support and the fruitful dicussions on the topic of array signal processing. He would also like to thank Dr. R. Pauli, Technische Universität München, for bringing [14] to his attention.

REFERENCES

[1] R. O. Schmidt, "Multiple emitter location and signal parameter estimation," in *Proc. RADC Spectrum Estimation Workshop*, 1986, pp. 243–258. reprinted in *IEEE Trans. Antennas Propagat.*, vol. AP-34, pp. 276–280, 1986.

[2] R. Kumaresan and D. W. Tufts, "Estimating the angles of arrival of multiple plane waves," *IEEE Trans. Aerosp. Electron. Syst.*, vol. AES-19, pp. 134–139, 1983.

[3] R. Roy and T. Kailath, "ESPRIT—Estimation of signal parameters via rotational invariance techniques," *IEEE Trans. Acoust., Speech, Signal Processing*, vol. 37, pp. 984–995, July 1989.

[4] M. Viberg, B. Ottersten, and T. Kailath, "Detection and estimation in sensor arrays using weighted subspace fitting," *IEEE Trans. Signal Processing*, vol. 39, pp. 2436–2449, Nov. 1991.

[5] P. Comon and G. H. Golub, "Tracking a few extreme singular values and vectors in signal processing," *Proc. IEEE*, vol. 78, pp. 1327–1343, Aug. 1990.

[6] B. Yang, "Projection approximation subspace tracking," *IEEE Trans. Signal Processing*, vol. 43, pp. 95–107, Jan. 1995.

[7] G. H. Golub and C. F. VanLoan, *Matrix Computations*, 3rd ed. Baltimore, MD: Johns Hopkins Univ. Press, 1996.

[8] J. R. Bunch, C. P. Nielsen, and D. Sorenson, "Rank-one modification of the symmetric eigenproblem," *Numer. Math.*, vol. 31, pp. 31–48, 1978.

[9] I. Karasalo, "Estimating the covariance matrix by signal subspace averaging," *IEEE Trans. Acoust., Speech, Signal Processing*, vol. ASSP-34, pp. 8–12, Jan. 1986.

[10] E. Oja, "A simplified neuron model as a principal component analyzer," *J. Math. Biol.*, vol. 15, pp. 267–273, 1982.

[11] J. Yang and M. Kaveh, "Adaptive eigensubspace algorithms for direction or frequency estimation and tracking," *IEEE Trans. Acoust., Speech, Signal Processing*, vol. 36, pp. 241–251, Feb. 1988.

[12] R. Weber, "Subspace Tracking for Mobile Communications," Techn. Univ. München, Munich, Germany, Tech. Rep. TUM-LNS-TR-97-7, 1997.

[13] R. Weber and J. A. Nossek, "Efficient DOA tracking for TDMA-based SDMA mobile communications," *Proc. IEEE Veh. Technol. Conf.*, pp. 2099–2103, 1999.

[14] D. Agrawal, T. J. Richardson, and R. Urbanke, "Packings in complex grassmannian space and their use as multiple-antenna signal constellations," Bell Laboratories, Lucent Technologies, Murray Hill, NJ, 1999. Internal Tech. Memo..

[15] W. Givens, "Computation of plane unitary rotations transforming a general matrix to triangular form," *J. Soc. Ind. Appl. Math.*, vol. 6, no. 1, pp. 26–50, 1958.

[16] PAL. N. Trefethen and D. Bau III, *Numerical Linear Algebra*. Philadelphia: SIAM, 1997.

[17] J. G. F Francis, "The QR transformation—A unitary analogue to the LR transformation—Part 1," *Comput. J.*, vol. 4, pp. 265–271, 1961.

[18] F. D. Murnaghan, "The topology of the real n-dimensional rotation group," in *The Theory of Group Representations*. Baltimore, MD: Johns Hopkins Univ. Press, 1938, ch. X.5, pp. 318–325.

[19] ——, *The Unitary and Rotation Groups Vol. III of Lectures on Applied Mathematics*. New York: Spartan, 1962.

[20] D. Fuhrmann, A. Srivastava, and H. Moon, "Subspace tracking via rigid body dynamics," *Proc. 6th IEEE SP Workshop Statist. Signal Array Process.*, 1996.

[21] D. Fuhrmann, "A geometric approach to subspace tracking," in *Proc. 31st Asilomar Conf. Signals, Syst., Comput.*, vol. 1, 1998.

[22] J.-M. Delosme, "CORDIC algorithms: Theory and extensions," in *Proc. SPIE Adv. Algorithms Arch. Signal Process.*, vol. 4, 1989, pp. 131–145.

[23] Tms320c6701 Digital Signal Processor Datasheet (sprs067) [Online]. Available: http://www.ti.com/sc/docs/products/dsp/tms320c6701.html #Datasheets

[24] M. Haardt, M. D. Zoltowski, C. P. Mathews, and J. A. Nossek, "2D Unitary ESPRIT for efficient 2D parameter estimation," *Proc. IEEE Int. Conf. Acoust., Speech, Signal Process.*, pp. 2096–2099, 1995.

[25] W. H. Press, B. P. Flannery, S. A. Teukolsky, and W. T. Vetterling, *Numerical Recipes in C*. Cambridge, U.K.: Cambridge Univ. Press, 1988.

[26] M. Treiber, T. Kurpjuhn, and W. Utschick, "Implementation of a high-resolution parameter estimating scheme on a DSP," Techn. Univ. München, Munich, Germany, Tech. Rep. TUM-LNS-TR-00-3, 2000.

[27] M. Wax and T. Kailath, "Detection of signals by information theoretic criteria," *IEEE Trans. Acoust., Speech, Signal Processing*, vol. ASSP-33, pp. 387–392, 1985.
[28] G. Xu, R. H. Roy, and T. Kailath, "Detection of number of sources via exploitation of centro-symmetry property," *IEEE Trans. Signal Processing*, vol. 42, pp. 102–112, Jan. 1994.
[29] D. Fuhrmann, "Gradient flows on projection matrices for subspace estimation," in *Proc. 31st Asilomar Conf. Signals, Syst., Comput.*, vol. 2, 1998.
[30] A. Srivastava, "Geometric filtering for subspace tracking," *Proc. 1st IEEE SP Workshop Sensor Array Multichannel Process.*, vol. 2, 2000.
[31] W. Utschick and C. Brunner, "Efficient tracking and feedback of DL-eigenbeams in WCDMA," presented at the Fourth Eur. Personal Mobil Commun. Conf., Vienna, Austria, 2001.
[32] C. Brunner, W. Utschick, and J. A. Nossek, "Exploiting the short-term and long-term channel properties in space and time: Eigenbeamforming concepts for the BS in WCDMA," *Eur. Trans. Telecommun.*, vol. 5, pp. 365–378, 2001.

Wolfgang Utschick completed several industrial education programs before he received the diploma degree, summa cum laude, in electrical engineering in 1993 and the Dr.-Ing. degree, summa cum laude, in 1998, both from the Technische Universität München (TU München), Munich, Germany.

He has published several conference and journal papers in the field of neural computation, where he studied the design of error-correcting classification systems, and in the field of adaptive array processing, where he focuses on the physical layer of wireless communication systems. During the summer of 2000, he was a Visiting Researcher with the Eidgenössische Technische Hochschule, Zürich, Switzerland. He is currently a Research Scientist, Lecturer, and Head of the Signal Processing Research Group at the Institute of Circuit Theory and Signal Processing, TU München, as well as an Industrial Consultant in the field of third-generation mobile communication systems. His main research interests are signal processing in wireless communications, estimation theory, and nonlinear optimization.